

Structural Analysis of Wind Turbine Blade

Ayush Pandey, Adik Yadao

Dept. of Mechanical Engineering, G. H. Raisoni College of Engineering and Management, Maharashtra, India

Abstract - This study focuses on the structural analysis and design optimization of wind turbine blades to enhance efficiency, reliability, and cost-effectiveness. Wind turbine blades experience complex loads, including aerodynamic forces, gravitational effects, and extreme weather conditions. Ensuring their durability and maximizing energy capture efficiency is crucial for sustainable wind energy systems. Finite element analysis (FEA) is employed to evaluate stress distribution, deflection, natural frequencies, and failure modes such as buckling, delamination, and fatigue. The study compares conventional glass-fiber-reinforced composites with advanced carbon-fiber-reinforced composites to determine optimal material choices for strength, weight, and cost balance.

Optimization techniques, including genetic algorithms and gradient-based methods, refine blade design parameters such as length, airfoil shape, chord distribution, and twist angle. These approaches aim to minimize blade mass while maintaining structural integrity and performance. Material distribution is also optimized to enhance recyclability and sustainability. Manufacturing constraints and cost considerations are integrated into the design process, exploring innovations like hybrid materials and adaptive structures. The findings contribute to the development of next-generation wind turbine blades, supporting the expansion of efficient and sustainable wind energy solutions.

1. INTRODUCTION

Windmills, iconic structures of ingenuity and sustainability, have graced landscapes for centuries as symbols of innovation and utility. These remarkable machines harness the power of wind to perform essential tasks, making them a cornerstone of human development and a testament to our relationship with nature. Originating over a thousand years ago, windmills were initially designed to grind grain into flour and pump water, playing a vital role in agriculture and early industry.

At their core, windmills are marvels of mechanical engineering. Their sails or blades catch the wind's kinetic energy, converting it into rotational motion to power machinery. This simple yet effective principle underscores humanity's enduring quest to harness renewable resources. Over time, windmills evolved in design and purpose, from the traditional post and tower mills of

medieval Europe to the sleek, modern turbines generating clean electricity today.

Beyond their functional significance, windmills carry cultural and aesthetic value. They stand as picturesque landmarks in rural landscapes, often evoking a sense of nostalgia and harmony with the environment. In an era increasingly focused on sustainability, windmills—and their contemporary counterparts, wind turbines—underscore the importance of renewable energy in combating climate change.

Whether viewed as historical artifacts, practical tools, or symbols of a greener future, windmills inspire awe and remind us of humanity's ability to innovate in harmony with nature. Their story is a journey through time, intertwining tradition, technology, and an enduring reliance on the power of the wind.



Figure 1.1 – Windmills

Windmill blades are the defining feature of windmills, embodying the essence of harnessing wind energy and transforming it into mechanical or electrical power. These dynamic components, designed to capture the kinetic energy of the wind, are vital to the functionality and efficiency of windmills, both traditional and modern. Their evolution reflects centuries of engineering innovation and adaptation to changing needs and technologies.

The journey of windmill blades begins with their rudimentary wooden designs in early windmills, used primarily for grinding grain or pumping water. These

early blades were simple yet effective, leveraging basic aerodynamic principles to rotate and drive machinery. Over time, advancements in materials and understanding of wind dynamics revolutionized their design. Today, modern wind turbines are equipped with sleek, precision-engineered blades made of advanced composites like fiberglass and carbon fiber, designed to maximize energy capture while withstanding harsh environmental conditions.

Aerodynamic optimization plays a critical role in blade design, ensuring that they can generate power efficiently at varying wind speeds. From a cultural perspective, windmill blades are iconic, seen spinning atop historic mills in the European countryside or towering turbines on modern wind farms. Their visual presence often symbolizes humanity's ingenuity and commitment to sustainable energy.

As the demand for renewable energy grows, windmill blades stand at the forefront of innovation, enabling cleaner, greener solutions to power the world. They serve as both a bridge to the past and a beacon of progress, showcasing the harmonious integration of nature and technology.

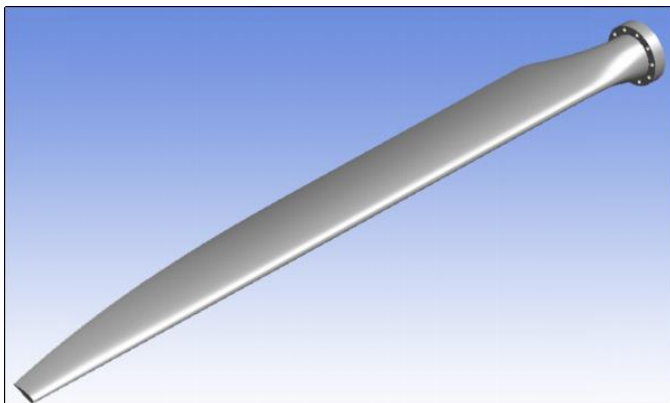


Figure 1.2- Windmill Blade

The size and number of blades vary depending on the windmill's purpose. For electricity generation, modern turbines often feature three blades for optimal balance, efficiency, and reduced noise. These blades are not only technological marvels but also represent the synergy between engineering and renewable energy innovation.

The design of windmill blades is a cornerstone of modern wind energy systems, directly influencing their efficiency, performance, and environmental impact. As the primary component responsible for capturing the kinetic energy of the wind, these blades are marvels of engineering, combining advanced materials and aerodynamic principles to optimize energy conversion.

A well-designed windmill blade maximizes energy capture by utilizing an airfoil shape, precision angles, and lightweight materials. The challenge lies in balancing strength, durability, and cost while ensuring the blades can endure harsh weather conditions and fluctuating wind loads over their lifespan. Modern innovations, such as smart materials and recyclable designs, have further advanced blade technology, making it integral to the global push for renewable energy.

Understanding the complexities of windmill blade design offers insight into the interplay between engineering ingenuity and environmental stewardship, driving the evolution of sustainable energy solutions.

The optimization of windmill blade design is essential for enhancing the efficiency, reliability, and sustainability of wind energy systems. As wind energy continues to play a critical role in transitioning to renewable energy, there is a growing need to maximize the performance of windmills while minimizing costs and environmental impacts.

2. Literature Review

Maalawi and Badr [1] examined the mechanical interaction between turbine blades and the electric generator, focusing on strategies for controlling pitch and rotational speed. Their study highlights the complexity of this problem, which involves numerous factors, relationships, and constraints. Designing optimal blades requires addressing aerodynamic, structural, and control challenges. Nevertheless, the design process can be effectively handled through an iterative and step-by-step approach. In aerodynamic optimization, the blade is modeled as a series of cross-sections along the pitch axis, with each section characterized by its airfoil profile, chord length, and attachment angle, influenced by both collective and local twist angles. Thresher and Dodge [2] explored how the blade's pitch angle is determined by the broader control strategy of the wind energy system. Accurately computing the airflow around rotating blades remains a highly complex task. Solving the three-dimensional Navier-Stokes equations within a rotating frame provides detailed insights into the wind flow and the forces exerted on the turbine surfaces, but the associated computational costs make this approach impractical for typical design and analysis work. Tangler [3] explained that the Blade Element Momentum (BEM) theory offers a simplified, one-dimensional approach to modeling blade aerodynamics. Despite its simplifications, it is widely used in the wind energy industry because it can predict blade performance with reasonable accuracy. United Technologies Corporation [4] conducted a comprehensive experimental modal analysis, employing a hydraulic shaker and multiple accelerometers to measure

one edgewise and two flapwise accelerations at approximately 20 blade stations. The resulting frequency response functions were compared to outcomes from a three-dimensional shell element finite element (FE) model. Their study focused on analyzing the dynamic characteristics associated with the seven lowest natural frequencies. Larsen and Kretz [5] utilized modal analysis techniques to identify dominant mode shapes in medium-sized wind turbine blades. Their approach successfully captured the primary modes related to the three lowest natural frequencies by analyzing the transfer function between a sinusoidal force applied at the blade tip and accelerometer responses recorded across up to 68 blade stations.

Larsen, Hansen, Baumgart, and Carlén [6] evaluated the dynamic behavior of wind turbine blades, including natural frequencies, damping ratios, and mode shapes, through modal analysis methods. Their work, conducted on the LM 19m blade, provides insights applicable to various blade designs. They assessed measurement reliability using standard deviations and coefficients of variation, noting high accuracy in natural frequencies and damping but greater variability in mode shape assessments. Primary deflection modes exhibited minimal uncertainty, whereas secondary, particularly torsional, deflections showed higher error margins. Although systematic errors such as blade support flexibility and sensor arrangement were acknowledged, they were not quantified. Dimitriadis [7] assessed the performance of Horizontal Axis Wind Turbines (HAWTs) using two analytical methods: Computational Fluid Dynamics (CFD) and Blade Element Momentum Theory (BEMT). He compared the results from both methods, conducting both two-dimensional and three-dimensional analyses to study the flow fields around turbine blades. Drag and lift coefficients were evaluated against available experimental data, revealing the superior accuracy and advantages of CFD modeling compared to BEMT. Dhurpate, Sutar, and Kale [8] analyzed the performance of a small horizontal-axis wind turbine rotor blade using various airfoil types. The study assumed low wind speeds and low Reynolds numbers, using a single airfoil type across the blade span. The rotor, with a 2-meter diameter and three blades, was modeled using four different airfoils, with a tip speed ratio of 7. Among all tested airfoils, the E387 airfoil demonstrated the best performance. Soland and Thuné [9] studied the rotor blade performance of a wind turbine with a diameter of 165 meters. They used computational tools such as XFLR5 and QBlade for simulations, applying the Blade Element Momentum Theory for analysis. Their findings detailed rotor performance under various operational loads and indicated that the NACA 63-6XX and NACA 64-6XX airfoils offered the best performance improvements compared to other tested airfoils. Kale,

Birajdar, and Sapali [10] designed new airfoil shapes to enhance wind turbine performance, creating distinct airfoils for the root and tip sections. They employed Blade Element Momentum Theory in designing a small wind turbine blade and conducted numerical analysis using QBlade software. Their results were compared with those for the NACA 2412 and SG 6042 airfoils, further comparing the performance of blades constructed with different individual airfoils using the same software. Mahri and Rouabah [11] conducted a dynamic stress evaluation on a wind turbine blade, which was designed using blade element theory. Their analysis incorporated beam theory for dynamic behavior and utilized both finite element modeling and blade motion equations to perform modal analysis. Edon [12] designed a 38-meter blade for a 1.5 MW wind turbine using the blade element momentum (BEM) theory. In his proposed future work, he introduced a chord distribution formula, which has been implemented in this study. Giguere and Selig [13] presented a methodology for optimizing blade geometry in wind turbine rotor design. Their approach utilized pre-programmed software tools to enhance both structural and cost-efficiency models. Jureczko, Pawlak, and Mezyk [14] applied BEM theory in blade design and used ANSYS software to calculate the blades' natural frequencies. Mode shapes were determined using a Timoshenko twisted, tapered beam element formulation. A genetic algorithm was employed to optimize the blade's performance by reducing vibrations, lowering costs, increasing output, and improving stability. Guo, Wu, Xu, and Li [15] developed a 1.5 MW wind turbine rotor with a 35-meter blade length using MATLAB. Their results confirmed the viability of MATLAB for large-scale turbine design, highlighting its cost-effectiveness in early-stage aerodynamic analysis and performance optimization. Computational fluid dynamics (CFD) results were used for validation. Carcangiu [16] utilized the FLUENT CFD tool to gain detailed insights into fluid flow behavior over wind turbine blades, contributing to more precise aerodynamic assessments. Jackson et al. [17] carried out a preliminary study for designing a 50-meter-long wind turbine blade using both fiberglass and carbon fiber composite materials. Adjustments in cross-sectional thickness were made to improve structural performance, and aerodynamic analyses were conducted for both clean and contaminated surface conditions. Wang et al. [18] investigated turbines of three different sizes to develop a cost-optimization model that maximized annual energy output. By using an enhanced BEM model integrated with blade structural dynamics, they successfully demonstrated reduced energy production costs.

Karam and Hani [19] implemented a multi-dimensional optimization technique to maximize the blade's natural frequency. The optimization process considered

parameters such as cross-sectional area, radius of gyration, and chord length, and the approach proved to be computationally efficient. Hsu [20] developed a theoretical framework for analyzing twisted, tapered beams using the spline collocation method. The provided expressions for cross-sectional area and moment of inertia are used as a basis in this work. Rao and Gupta [21] analyzed twisted, tapered, rotating Timoshenko beams using the finite element method. They derived the stiffness and mass matrices through shape functions and determined the natural frequencies by reformulating the problem into an eigenvalue analysis. Hillemer et al. [22] designed wind turbines with power outputs exceeding 5 MW by scaling existing rotor models. Using simple beam theory, they assessed stresses, bending moments, and natural frequencies. To reduce blade weight, airfoil shell thicknesses, as well as web and flange dimensions, were adjusted across sections, constrained by requirements for structural strength and minimal mass. Gooden [23] studied the two-dimensional aerodynamic properties of the FX 66 S 196 V1 airfoil, which is used in this report. The investigation focused on lift and drag coefficients over various Reynolds numbers. Bharath [24] designed a 45-meter blade for a wind speed of 12 m/s using BEM theory, calculating flow angles, thrust, torque, and power. The blade was modeled as a hollow tapered beam, with stiffness and mass matrices derived from the cross-sectional area and moment of inertia. Chord length dictated the taper, and airfoil thickness defined the height. Natural frequencies were evaluated in both axial and transverse directions. Optimization using MATLAB's *fmincon* function focused on maximizing power and minimizing mass under different constraint scenarios, yielding optimized chord profiles and performance visualizations. Miller et al. [25] provided an overview of recent advances in simulation techniques, tools, and applications for wind energy. The industry increasingly depends on CFD to design innovative turbines, though BEM remains more prevalent in early design phases due to its simplicity. They emphasized the need for new tools that integrate CFD earlier in the process and highlighted the role of algorithmic optimization in minimizing reliance on trial-and-error methods.

Madsen et al. [26] and parallel studies using blade-resolved rotor models often excluded hub geometry, yet CFD techniques successfully captured spanwise and tip flow patterns. These flow features significantly influence aerodynamic loads both within and outside the rotor plane. Horcas et al. [27] found that tools like HAWC2, based on OpenFAST physics models, tend to overestimate loads on 10 MW turbines at sub-rated wind speeds. Moreover, these tools often underestimate the performance benefits of curved blade tips. Due to their reliance on fixed drag polars and limitations in gradient

calculations, their effectiveness for optimization is reduced, especially when refining airfoil shapes. Batay et al. [28] demonstrated that aerostructural optimization can enhance wind turbine blade performance by reducing blade mass, which contributes to higher energy output and cost savings. They recommended future work focus on improving optimization techniques and expanding them to a wider range of turbine types. Jureczko, Pawlak, and Mezyk [29] created a general-purpose numerical model for wind turbine blade optimization and developed a software tool for multi-objective discrete-continuous optimization. Using ANSYS parametric modeling, users can vary blade thickness and key dimensions. The tool incorporates a modified genetic algorithm to optimize performance based on multiple objectives under specified constraints. Chattot [30] argued that while an optimal rotor does not strictly meet the Betz limit at each blade section, it does satisfy the condition on average across the Trefftz plane. The optimization problem remains well-posed in inviscid flow as long as the airfoil's maximum lift coefficient is respected. The study concluded that viscous effects have minor influence on the ideal blade shape, mainly reducing overall efficiency. The method is adaptable to geometric constraints, such as optimizing for a given chord distribution. Fuglsang and Madsen [31] introduced a direct design method for horizontal-axis wind turbines, employing numerical optimization and various computational models. These included aerodynamic, structural, aeroelastic (time-domain), extreme load, and noise prediction analyses. They also estimated manufacturing costs based on design loads. Jureczko, Pawlak, and Mezyk [32] (in a follow-up study) again emphasized their optimization software, capable of creating diverse blade models through ANSYS scripting. The tool applies a modified genetic algorithm for optimizing blades against several criteria under various constraints.

Schubel and Crossley [33] noted that the three-blade horizontal-axis configuration dominates today's wind turbine market due to its efficiency, control, and scalability. Supported by a global supply network, this design continues to outperform alternatives. Blade geometries are carefully shaped to enhance aerodynamics, with increasing width, twist, and thickness near the hub to withstand higher bending moments. While current innovations focus on scaling turbine size, future advancements may prioritize performance enhancements via new materials and airfoil designs, especially as physical growth reaches practical limits.

3. Design of the blade

The model as provided by Eleation has the dimensions as shown in 'Figure 3.1'. It is made from aluminum alloy, it

provides a lightweight yet durable structure with excellent corrosion resistance. This windmill blade is designed for small-scale wind energy applications. The total length of the blade is 9500mm.

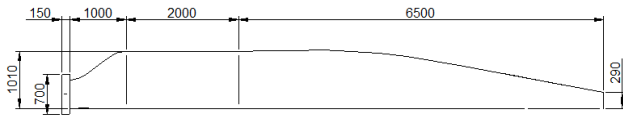


Figure 3.1- Blade Dimensions

The 'Figure 3.2' shows the aerofoil geometry of the windmill blade. The total width of the blade is 1010mm whereas the maximum thickness is 214mm. This blades has a gradual twist from root to tip.

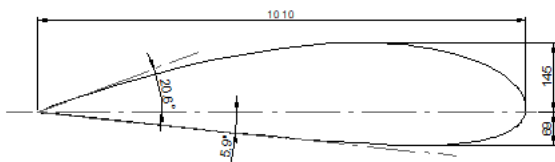


Figure 3.2- Blade Aerofoil Shape

4. Methodology

Methodology of this project consists of following points as guided by the Eleation team.

i. Initial Blade Geometry:

- Aerofoil shape to be used for the blade's initial shape.

ii. Material Selection:

- Aluminium alloys.

iii. Mesh Selection:

- Hexagonal mesh
- Mesh size - 45mm

'Figure 4.1' below shows the meshed wind turbine blade, here primary hexagonal mesh of size 45mm is used. There are 26958 nodes and 109511 elements in the meshed wind turbine blade. There are tria elements only where it is necessary; all others are tetra elements.

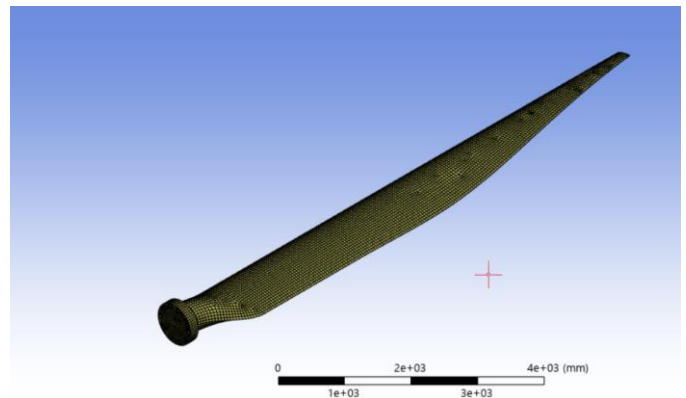


Figure 4.1- Meshed Blade

4.1. Transient Structural Analysis:

Transient Structural Analysis is a finite element analysis technique used to evaluate a structure's response to time-dependent loads, displacements, or environmental conditions. It accounts for inertia and damping effects, making it essential for studying impact, vibrations, and shock loads. It employs explicit methods for short-duration, high-speed events and implicit methods for long-duration, gradual changes. Applications include earthquake-resistant buildings and shock-wave effects on structures. By incorporating time-dependent boundary conditions, transient analysis ensures more accurate and realistic structural performance predictions.

- Max Pressure: 101325 Pa;
- Apply pressure on the blade and constraint the end locations i.e, holes
- Perform the analysis for 100 sec.

'Figure 4.2' shows that the pressure of 101325 Pa, which is atmospheric pressure is applied on the face of the wind turbine blade and the bolting holes have been fixed for the transient structural analysis of the blade. The analysis is performed for 100 sec, and the results are as shown below.

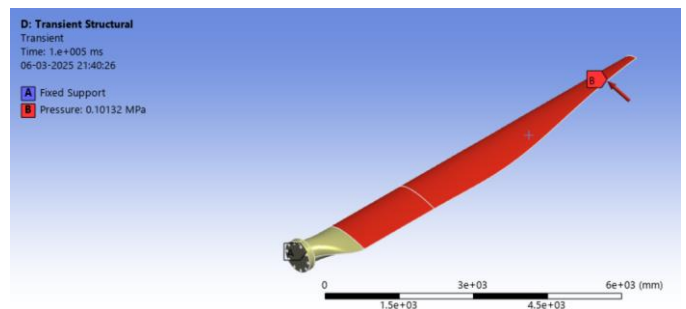


Figure 4.2- Transient Structural Analysis loading on Blade

Output:

- Stress

'Figure 4.3' shows that the minimum stress developed during the transient structural analysis is 0.076301 MPa, it occurs at the tip of the wind turbine blade. Whereas maximum stress developed during the transient stress analysis is 649.12 MPa, it occurs at the neck of the blade.

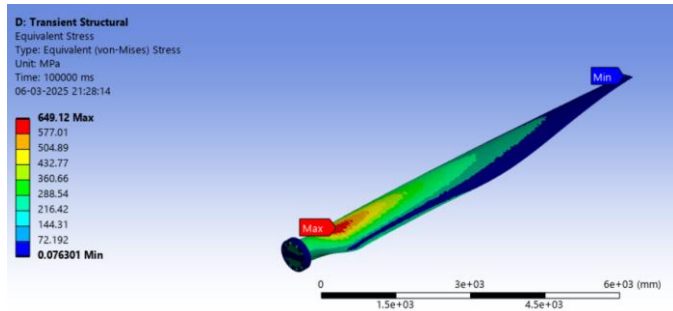


Figure 4.3- Von-Mises Stress- 649.12 MPa

- Deformation

'Figure 4.4' shows that the minimum deformation during the transient structural analysis is 0mm, it occurs at the bolting holes of the wind turbine blade. Whereas maximum deformation during the transient stress analysis is 1894.4mm, it occurs at the tip of the blade.

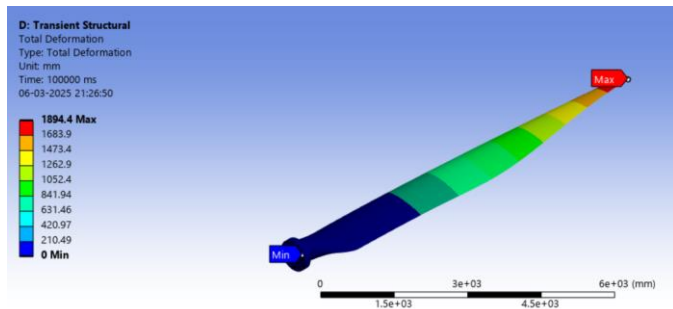


Figure 4.4- Deformation- 1894.4mm

- Strain

'Figure 4.4' shows that the minimum strain during the transient structural analysis is 1.1877×10^{-6} , it occurs at the tip of the wind turbine blade. Whereas maximum strain during the transient stress analysis is 0.009193, it occurs at the neck of the blade.

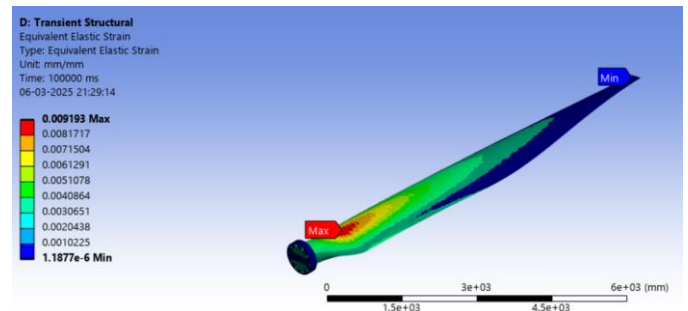


Figure 4.5- Strain- 0.009193

- FOS

'Figure 4.4' shows that the minimum factor of safety during the transient structural analysis is 0.43135, it occurs at the neck of the wind turbine blade. Whereas maximum factor of safety during the transient stress analysis is 15, it occurs at the bolting holes of the blade.

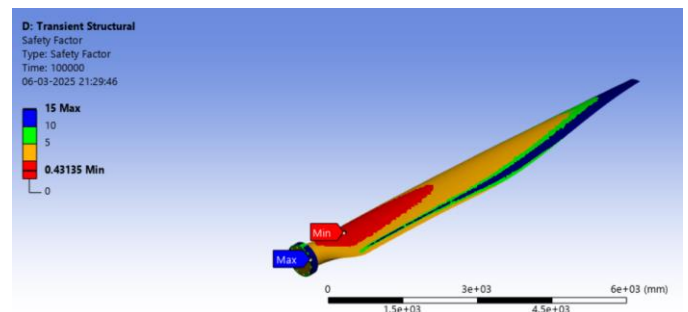


Figure 4.6- FOS- 0.43135

4.2. Static Structural Analysis:

Static Structural Analysis determines a structure's response to constant or slowly varying loads, assuming no inertia or damping effects. It ensures equilibrium by analyzing stresses, strains, and deformations under forces, pressure, thermal effects, and constraints. Used in civil, automotive, aerospace, and mechanical engineering, it evaluates load-bearing capacity, material strength, and failure risks. There are linear (small deformations, proportional behavior) and nonlinear (plasticity, large deformations, contact interactions) approaches. This analysis is essential for designing safe, efficient structures like buildings, bridges, and machinery, ensuring they withstand applied forces without excessive deformation.

- Max Pressure: 101325 Pa;
- Apply pressure on the blade and constraint the end locations i.e., holes

'Figure 4.7' shows that the pressure of 101325 Pa, which is atmospheric pressure, is applied on the face of the wind turbine blade and the bolting holes have been fixed for the

static structural analysis of the blade. The results of the analysis are as shown below.

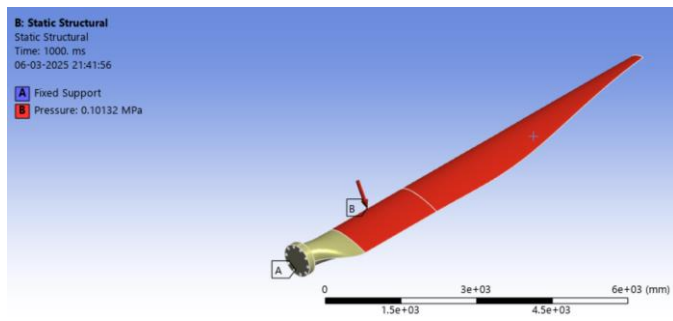


Figure 4.7- Static Structural Analysis loading on Blade

Output:

- Stress

'Figure 4.8' shows that the minimum stress developed during the static structural analysis is 0.076551 MPa, it occurs at the tip of the wind turbine blade. Whereas maximum stress developed during the transient stress analysis is 652.35 MPa, it occurs at the neck of the blade.

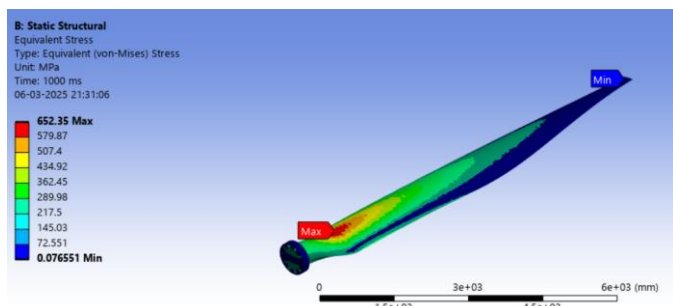


Figure 4.8- Von-Mises Stress- 652.35 MPa

- Deformation

'Figure 4.9' shows that the minimum deformation during the static structural analysis is 0mm, it occurs at the bolting holes of the wind turbine blade. Whereas maximum deformation during the transient stress analysis is 1904.1mm, it occurs at the tip of the blade.

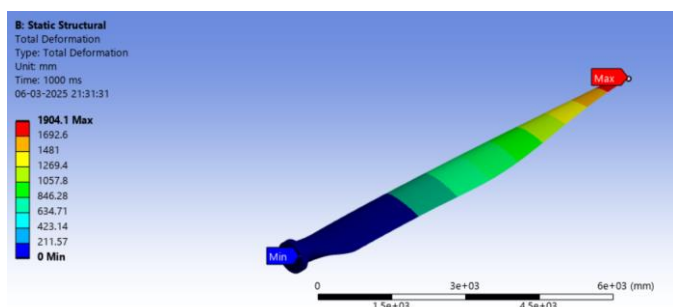


Figure 4.9- Deformation- 1904.1mm

- Strain

'Figure 4.10' shows that the minimum strain during the static structural analysis is 1.1908×10^{-6} , it occurs at the tip of the wind turbine blade. Whereas maximum strain during the transient stress analysis is 0.0092361, it occurs at the neck of the blade.

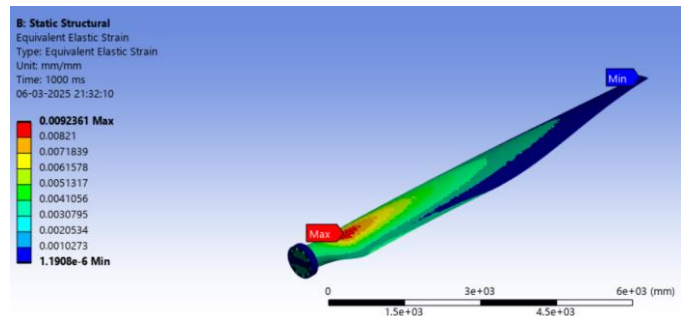


Figure 4.10- Strain- 0.0092361

- FOS

'Figure 4.11' shows that the minimum factor of safety during the static structural analysis is 0.42922, it occurs at the neck of the wind turbine blade. Whereas maximum factor of safety during the transient stress analysis is 15, it occurs at the bolting holes of the blade.

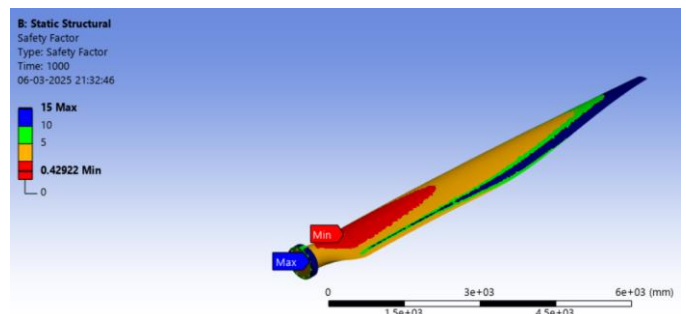


Figure 4.11- FOS- 0.42922

4.3. Modal Analysis:

Modal Analysis determines a structure's natural frequencies and mode shapes, essential for understanding vibration characteristics. It helps prevent resonance, which can cause structural failure. This analysis assumes no external forces, focusing on how the structure vibrates due to inherent properties like stiffness and mass. Used in aerospace, automotive, civil, and mechanical engineering, it ensures safety in bridges, engines, and machinery. Modal analysis can be theoretical or numerical. It's crucial for optimizing designs, reducing unwanted vibrations, and improving structural stability under dynamic conditions like earthquakes, machinery operation, or vehicle motion.

- Perform Modal Analysis with pre-stress condition as Static Structural analysis.

- Max Frequency: 300Hz

'Figure 4.12' shows that the modal analysis is done on the wind turbine blade for the maximum frequency of 300 Hz, keeping the static structural analysis performed on the blade as the prestress condition. Here we find the first six modes of natural frequency and their respective displacements.

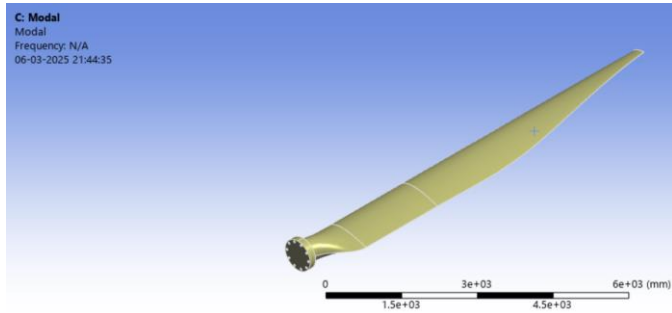


Figure 4.12- Modal Analysis

Output:

1. Mode 1

'Figure 4.13' shows that the first mode of natural frequency occurs at 2.9614 Hz. Here minimum deformation is 0mm, it occurs at the bolting holes of the wind turbine blade. Whereas maximum deformation is 1.6483mm, it occurs at the tip of the blade.

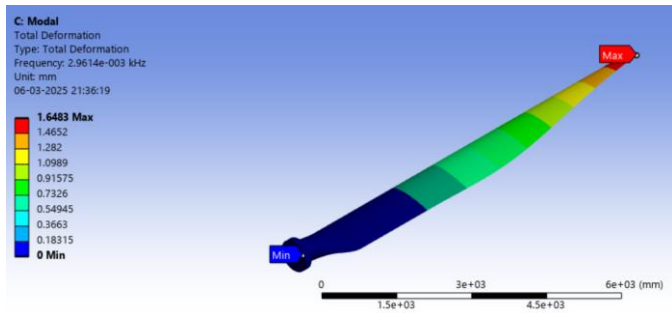


Figure 4.13- Mode 1

2. Mode 2

'Figure 4.14' shows that the second mode of natural frequency occurs at 9.140 Hz. Here minimum deformation is 0mm, it occurs at the bolting holes of the wind turbine blade. Whereas maximum deformation is 1.4954mm, it occurs at the tip of the blade.

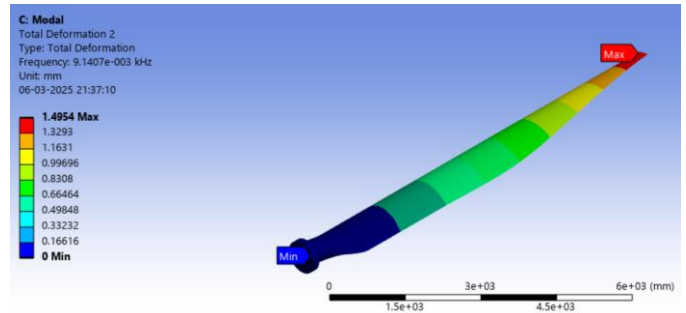


Figure 4.14- Mode 2

3. Mode 3

'Figure 4.15' shows that the third mode of natural frequency occurs at 14.202 Hz. Here minimum deformation is 0mm, it occurs at the bolting holes of the wind turbine blade. Whereas maximum deformation is 2.751mm, it occurs at the tip of the blade.

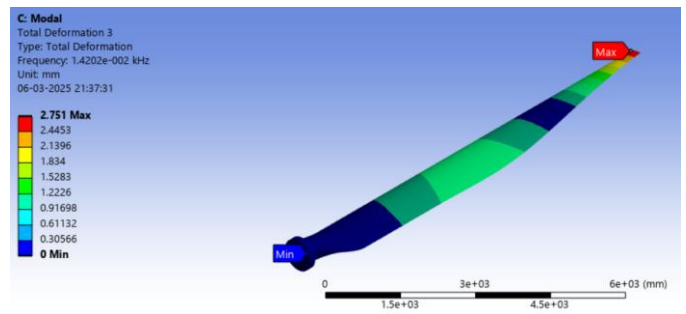


Figure 4.15- Mode 3

4. Mode 4

'Figure 4.16' shows that the fourth mode of natural frequency occurs at 31.533 Hz. Here minimum deformation is 0mm, it occurs at the bolting holes of the wind turbine blade. Whereas maximum deformation is 3.5472mm, it occurs at the tip of the blade.

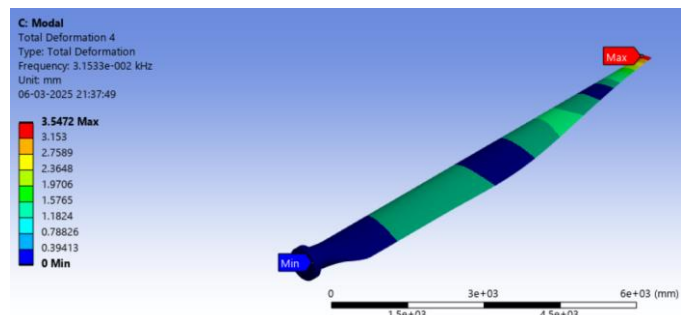


Figure 4.16- Mode 4

5. Mode 5

'Figure 4.17' shows that the fifth mode of natural frequency occurs at 47.869 Hz. Here minimum deformation is 0mm, it occurs at the bolting holes of the

wind turbine blade. Whereas maximum deformation is 2.5114mm, it occurs at the tip of the blade.

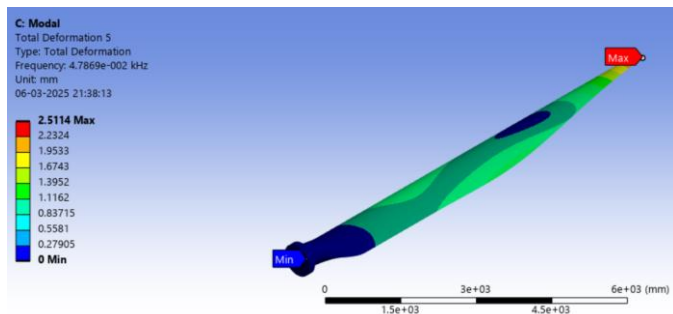


Figure 4.17- Mode 5

6. Mode 6

'Figure 4.18' shows that the sixth mode of natural frequency occurs at 55.224 Hz. Here minimum deformation is 0mm, it occurs at the bolting holes of the wind turbine blade. Whereas maximum deformation is 1.7743mm, it occurs at the tip of the blade.

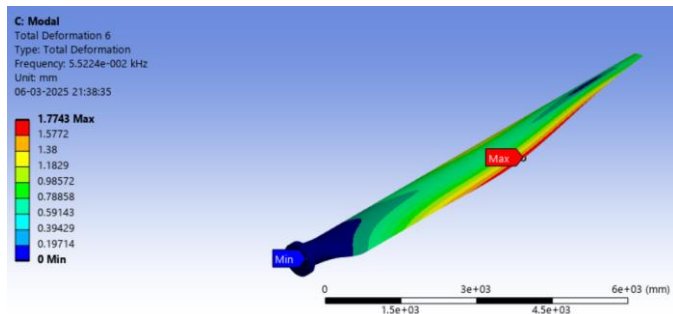


Figure 4.18- Mode 6

5. Design Modification

I modified the wind turbine blade by increasing its thickness, which enhanced structural strength and aerodynamic performance. Thicker blades provide greater stiffness, reducing deformation under high wind loads and improving durability. This modification also allowed for better load distribution, minimizing stress concentrations along the blade span. All this is done maintaining an optimal thickness-to-chord ratio. Following drawing shows the modified aerofoil shape of the blade.

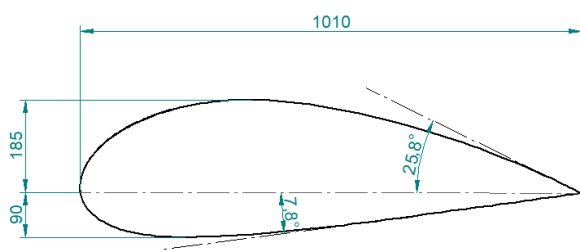


Figure 5.1- Modified Blade Aerofoil Shape

The above 'Figure 5.1' shows that the thickness of the aerofoil shape of the wind turbine blade has increased to 275mm whereas earlier it was 214mm keeping the width of the blade at 1010mm. This implies that the thickness to chord ratio changed from 21.1% in the initial design to 27.2% in the modified design of the wind turbine blade. Thus, the new design is 6.1% thicker than the initial blade design. The angle at the edge also changes significantly initially from 26.5° to 33.6° in the modified wind turbine blade design.

'Figure 5.2' below shows the meshed wind turbine blade, here primary hexagonal mesh of size 45mm is used. There are 29263 nodes and 120995 elements in the meshed wind turbine blade. There are tria elements only where it is necessary; all others are tetra elements.

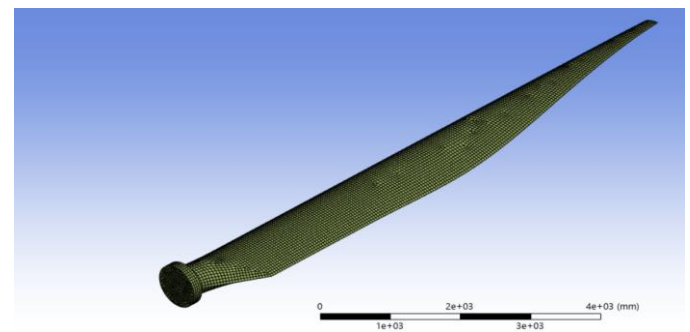


Figure 5.2- Meshed Blade

5.1. Transient Structural Analysis:

- Max Pressure: 101325 Pa;
- Apply pressure on the blade and constraint the end locations i.e, holes
- Perform the analysis for 100 sec.

'Figure 5.3' shows that the pressure of 101325 Pa, which is atmospheric pressure, is applied on the face of the wind turbine blade and the bolting holes have been fixed for the transient structural analysis of the blade. The analysis is performed for 100 sec, and the results are as shown below.

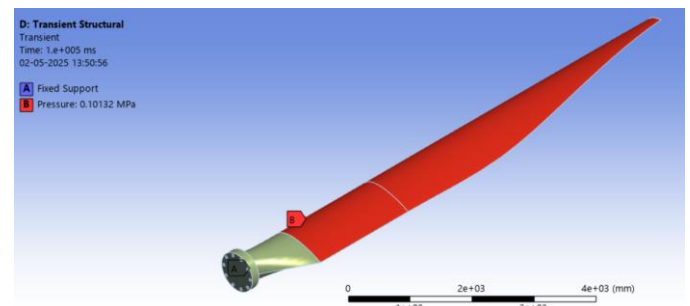


Figure 5.3- Transient Structural Analysis loading on Blade

Output:

- Stress

'Figure 5.4' shows that the minimum stress developed during the transient structural analysis is 0.059351 MPa, it occurs at the tip of the wind turbine blade. Whereas maximum stress developed during the transient stress analysis is 418.63 MPa, it occurs at the neck of the blade.

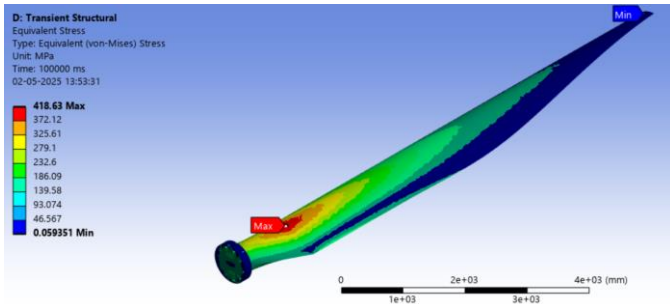


Figure 5.4- Von-Mises Stress- 652.35 MPa

- Deformation

'Figure 5.5' shows that the minimum deformation during the transient structural analysis is 0mm, it occurs at the bolting holes of the wind turbine blade. Whereas maximum deformation during the transient stress analysis is 980.44mm, it occurs at the tip of the blade.

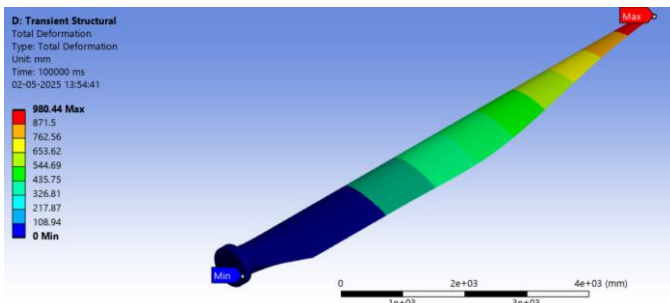


Figure 5.5- Deformation- 980.44mm

- Strain

'Figure 5.6' shows that the minimum strain during the transient structural analysis is 9.2356×10^{-7} , it occurs at the tip of the wind turbine blade. Whereas maximum strain during the transient stress analysis is 0.0072879, it occurs at the neck of the blade.

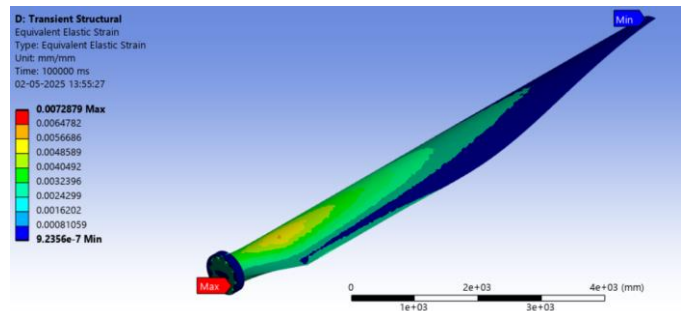


Figure 5.6- Strain- 0.0072879

- FOS

'Figure 5.7' shows that the minimum factor of safety during the transient structural analysis is 1.0749, it occurs at the neck of the wind turbine blade. Whereas maximum factor of safety during the transient stress analysis is 15, it occurs at the bolting holes of the blade.

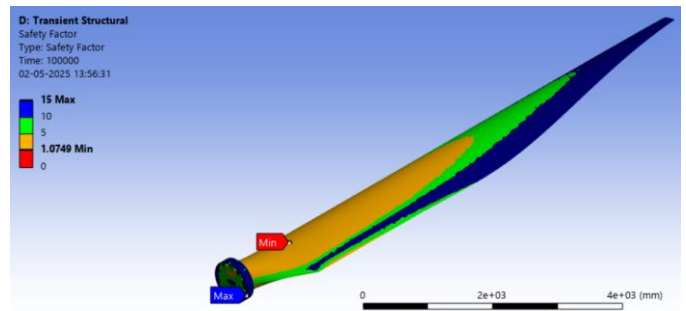


Figure 5.7- FOS- 1.0749

5.2. Static Structural Analysis:

- Max Pressure: 101325 Pa;
- Apply pressure on the blade and constraint the end locations i.e., holes

'Figure 5.8' shows that the pressure of 101325 Pa, which is atmospheric pressure, is applied on the face of the wind turbine blade and the bolting holes are fixed for the static structural analysis of the blade. The results of the analysis are as shown below.

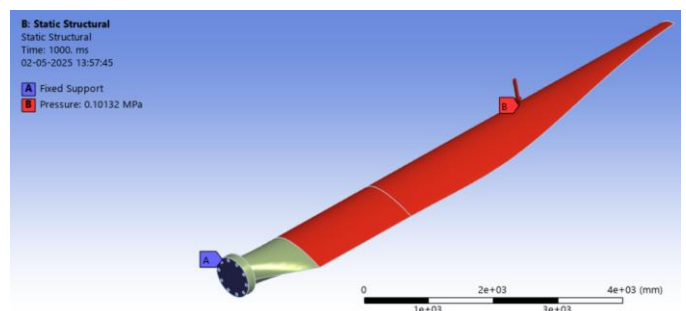


Figure 5.8- Static Structural Analysis loading on Blade

Output:

- Stress

'Figure 5.9' shows that the minimum stress developed during the static structural analysis is 0.059379 MPa, it occurs at the tip of the wind turbine blade. Whereas maximum stress developed during the transient stress analysis is 419.21 MPa, it occurs at the neck of the blade.

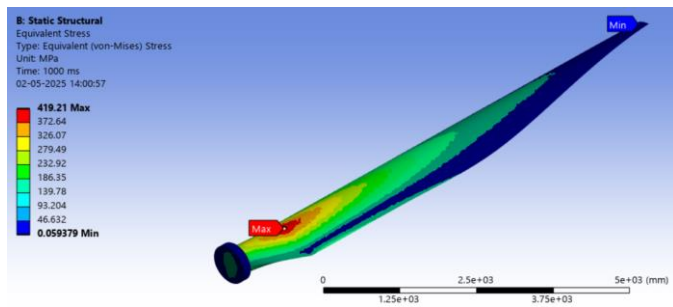


Figure 5.9- Von-Mises Stress- 419.21 MPa

- Deformation - 974.05mm

'Figure 5.10' shows that the minimum deformation during the static structural analysis is 0mm, it occurs at the bolting holes of the wind turbine blade. Whereas maximum deformation during the transient stress analysis is 974.05mm, it occurs at the tip of the blade.

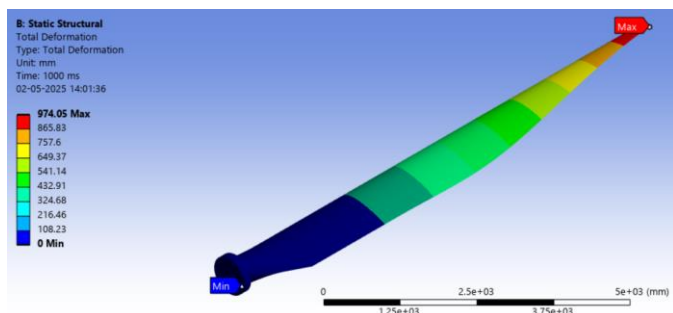


Figure 5.10- Deformation- 974.05mm

- Strain

'Figure 5.11' shows that the minimum strain during the static structural analysis is 9.2385×10^{-7} , it occurs at the tip of the wind turbine blade. Whereas maximum strain during the transient stress analysis is 0.005835, it occurs at the neck of the blade.

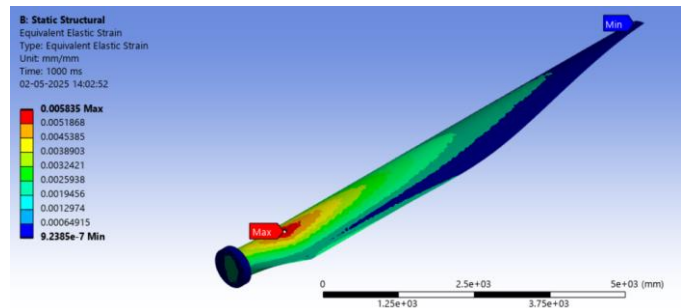


Figure 5.11- Strain- 0.005835

- FOS

'Figure 5.12' shows that the minimum factor of safety during the static structural analysis is 1.0734, it occurs at the neck of the wind turbine blade. Whereas maximum factor of safety during the transient stress analysis is 15, it occurs at the bolting holes of the blade.

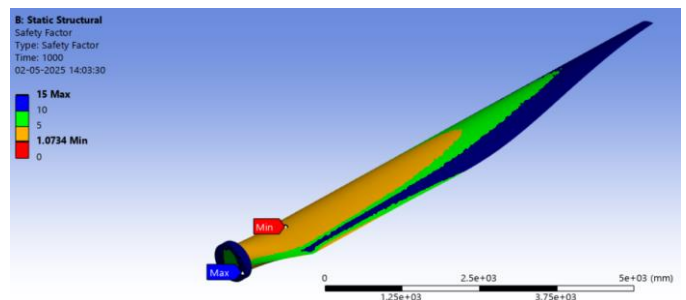


Figure 5.12- FOS- 1.0734

5.3. Modal Analysis:

- Perform Modal Analysis with pre-stress condition as Static Structural analysis.
- Max Frequency: 300Hz

'Figure 5.13' shows that the modal analysis is done on the wind turbine blade for the maximum frequency of 300 Hz, keeping the static structural analysis performed on the blade as the prestress condition. Here we find the first six modes of natural frequency and their respective displacements.

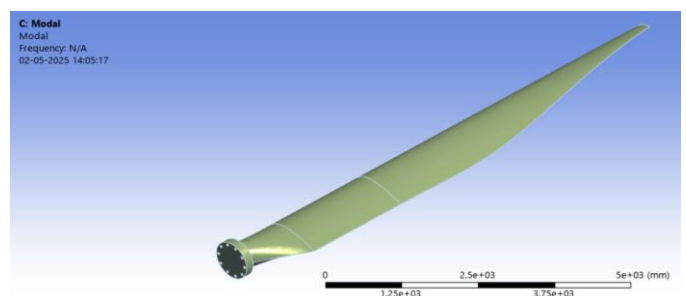


Figure 5.13- Modal Analysis

Output:

1. Mode 1

'Figure 5.14' shows that the first mode of natural frequency occurs at 3.6181 Hz. Here minimum deformation is 0mm, it occurs at the bolting holes of the wind turbine blade. Whereas maximum deformation is 1.4233mm, it occurs at the tip of the blade.

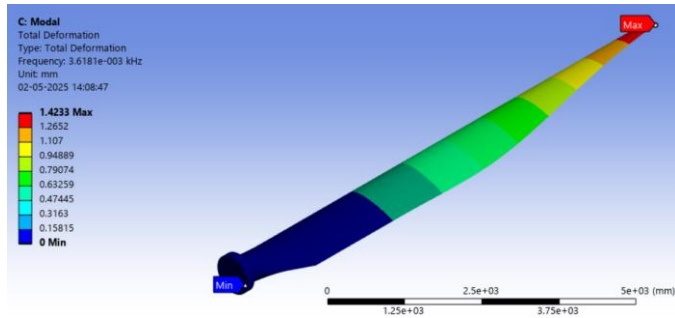


Figure 5.14- Mode 1

2. Mode 2

'Figure 5.15' shows that the second mode of natural frequency occurs at 9.0448 Hz. Here minimum deformation is 0mm, it occurs at the bolting holes of the wind turbine blade. Whereas maximum deformation is 1.3014mm, it occurs at the tip of the blade.

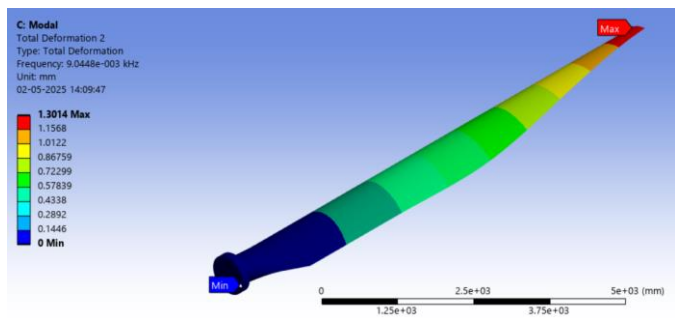


Figure 5.15- Mode 2

3. Mode 3

'Figure 5.16' shows that the third mode of natural frequency occurs at 17.334 Hz. Here minimum deformation is 0mm, it occurs at the bolting holes of the wind turbine blade. Whereas maximum deformation is 2.3998mm, it occurs at the tip of the blade.

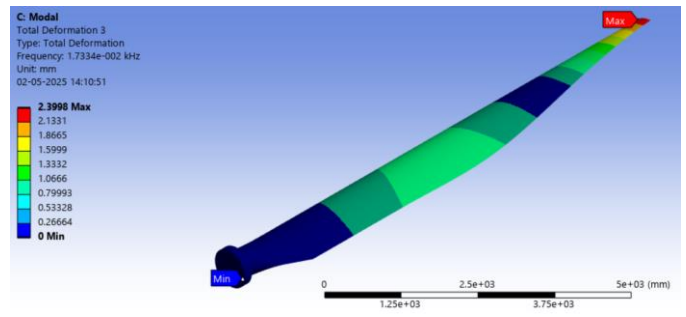


Figure 5.16- Mode 3

4. Mode 4

'Figure 5.17' shows that the fourth mode of natural frequency occurs at 37.166 Hz. Here minimum deformation is 0mm, it occurs at the bolting holes of the wind turbine blade. Whereas maximum deformation is 3.1889mm, it occurs at the tip of the blade.

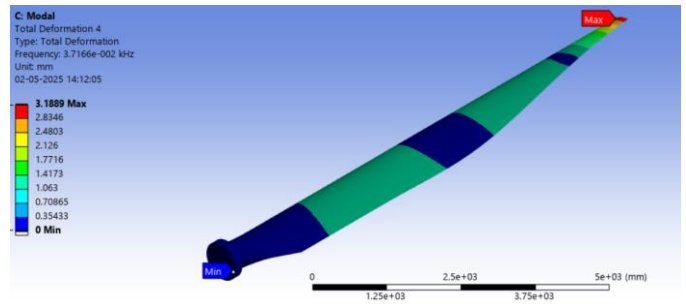


Figure 5.17- Mode 4

5. Mode 5

'Figure 5.18' shows that the fifth mode of natural frequency occurs at 49.699 Hz. Here minimum deformation is 0mm, it occurs at the bolting holes of the wind turbine blade. Whereas maximum deformation is 2.0397mm, it occurs at the tip of the blade.

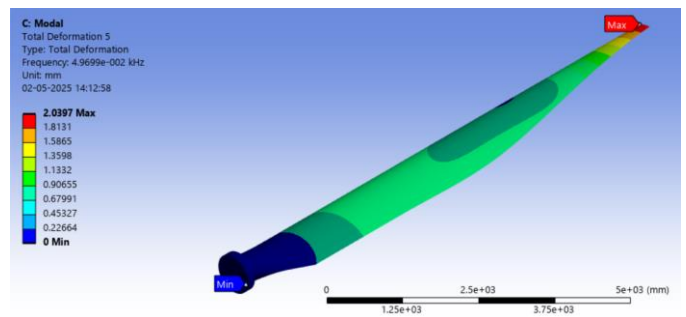


Figure 5.18- Mode 5

6. Mode 6

'Figure 5.19' shows that the sixth mode of natural frequency occurs at 64.456 Hz. Here minimum deformation is 0mm, it occurs at the bolting holes of the

wind turbine blade. Whereas maximum deformation is 1.6436mm, it occurs at the tip of the blade.

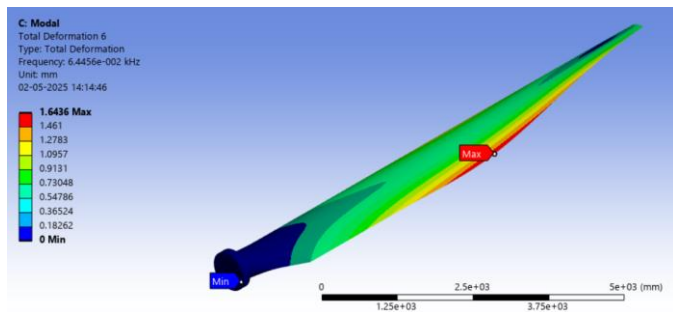


Figure 5.19- Mode 6

6. Carbon Fibre

Applied carbon fibre as a material to both initial and modified design profiles of the aerofoil and following are the results of the structural analysis.

6.1. Initial Design

i. Transient Structural Analysis:

- Max Pressure: 101325 Pa;
- Apply pressure on the blade and constraint the end locations i.e, holes
- Perform the analysis for 100 sec.

'Figure 6.1' shows that the pressure of 101325 Pa, which is atmospheric pressure, is applied on the face of the wind turbine blade and the bolting holes have been fixed for the transient structural analysis of the blade. The analysis is performed for 100 sec, and the results are as shown below.

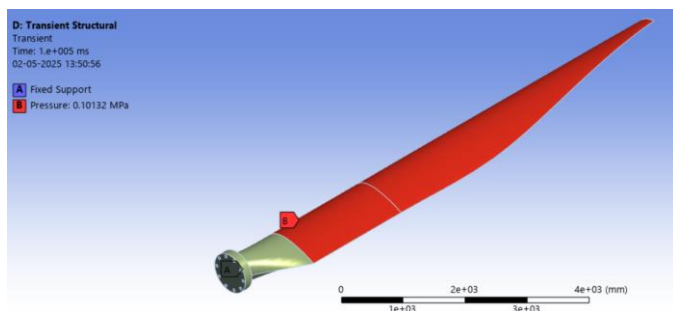


Figure 6.1- Transient Structural Analysis loading on Blade

Output:

- Stress

'Figure 6.2' shows that the minimum stress developed during the transient structural analysis is 0.08075 MPa, it occurs at the tip of the wind turbine blade. Whereas maximum stress developed during the transient stress analysis is 658.43 MPa, it occurs at the neck of the blade.

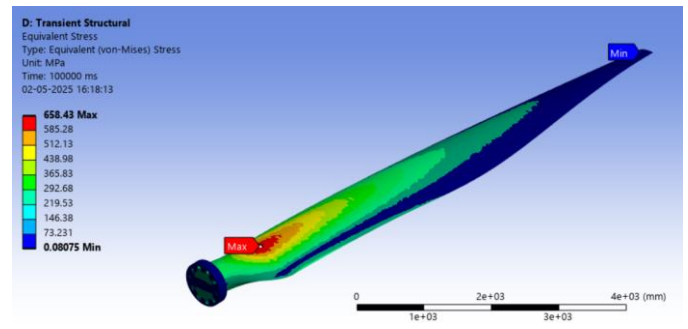


Figure 6.2- Von-Mises Stress- 658.43 MPa

- Deformation

'Figure 6.3' shows that the minimum deformation during the transient structural analysis is 0mm, it occurs at the bolting holes of the wind turbine blade. Whereas maximum deformation during the transient stress analysis is 908.49mm, it occurs at the tip of the blade.

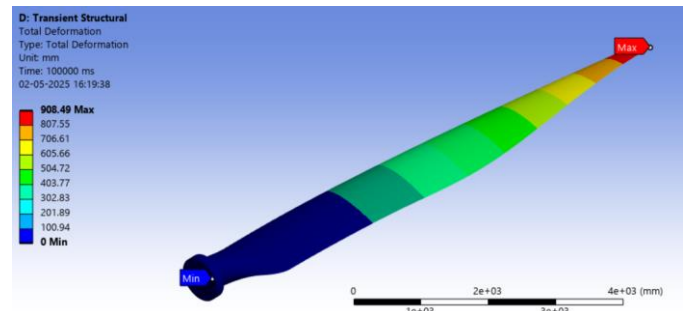


Figure 6.3- Deformation- 908.49mm

- Strain

'Figure 6.4' shows that the minimum strain during the transient structural analysis is 5.8153×10^{-7} , it occurs at the tip of the wind turbine blade. Whereas maximum strain during the transient stress analysis is 0.0044157, it occurs at the neck of the blade.

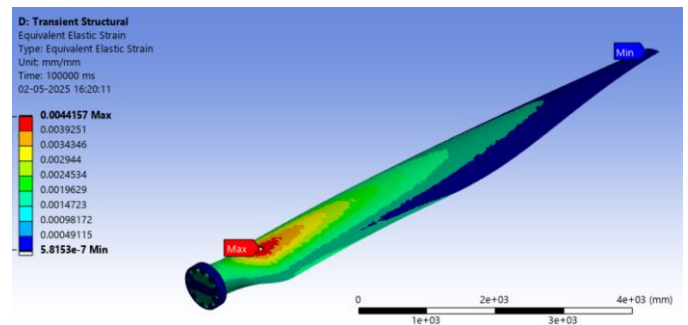


Figure 6.4- Strain- 0.0044157

- FOS

'Figure 6.5' shows that the minimum factor of safety during the transient structural analysis is 6.8344, it occurs at the neck of the wind turbine blade. Whereas maximum

factor of safety during the transient stress analysis is 15, it occurs at the bolting holes of the blade.

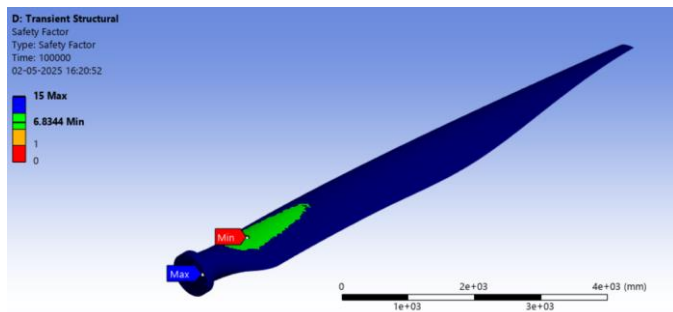


Figure 6.5- FOS- 6.8344

ii. **Static Structural Analysis:**

- Max Pressure: 101325 Pa;
- Apply pressure on the blade and constraint the end locations i.e., holes

'Figure 6.6' shows that the pressure of 101325 Pa, which is atmospheric pressure, is applied on the face of the wind turbine blade and the bolting holes are fixed for the static structural analysis of the blade. The results of the analysis are as shown below.

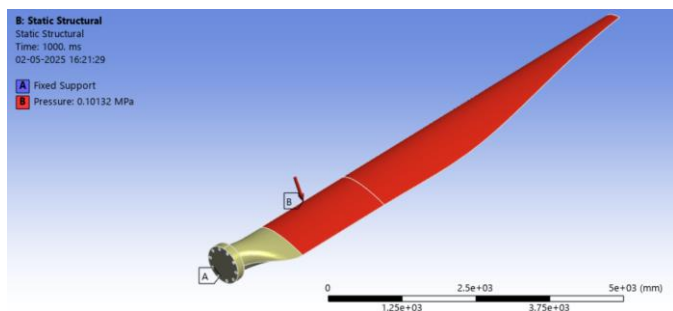


Figure 6.6- Static Structural Analysis loading on Blade

Output:

- Stress

'Figure 6.7' shows that the minimum stress developed during the static structural analysis is 0.080765 MPa, it occurs at the tip of the wind turbine blade. Whereas maximum stress developed during the transient stress analysis is 659.3 MPa, it occurs at the neck of the blade.

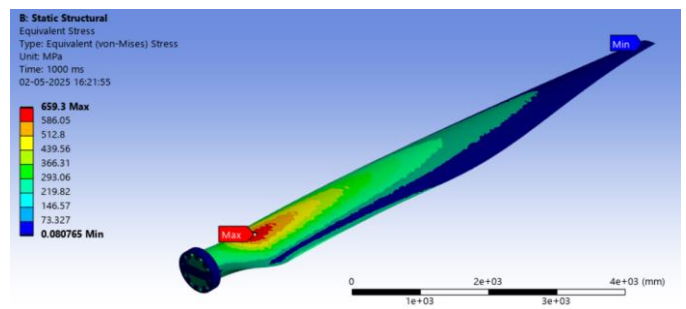


Figure 6.7- Von-Mises Stress- 659.3 MPa

- Deformation

'Figure 6.8' shows that the minimum deformation during the static structural analysis is 0mm, it occurs at the bolting holes of the wind turbine blade. Whereas maximum deformation during the transient stress analysis is 908.72mm, it occurs at the tip of the blade.

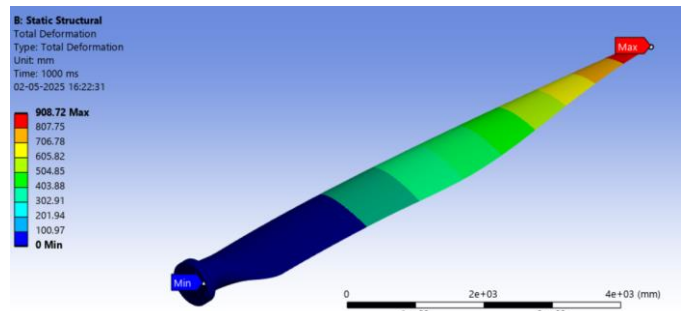


Figure 6.8- Deformation- 908.72mm

- Strain

'Figure 6.9' shows that the minimum strain during the static structural analysis is 5.817×10^{-7} , it occurs at the tip of the wind turbine blade. Whereas maximum strain during the transient stress analysis is 0.0044209, it occurs at the neck of the blade.

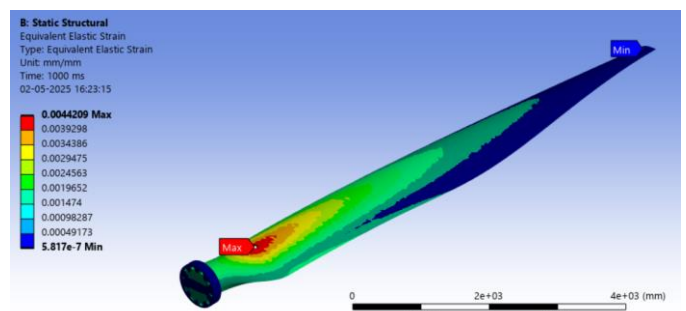


Figure 6.9- Strain- 0.0044209

- FOS

'Figure 6.10' shows that the minimum factor of safety during the static structural analysis is 6.8255, it occurs at the neck of the wind turbine blade. Whereas maximum

factor of safety during the transient stress analysis is 15, it occurs at the bolting holes of the blade.

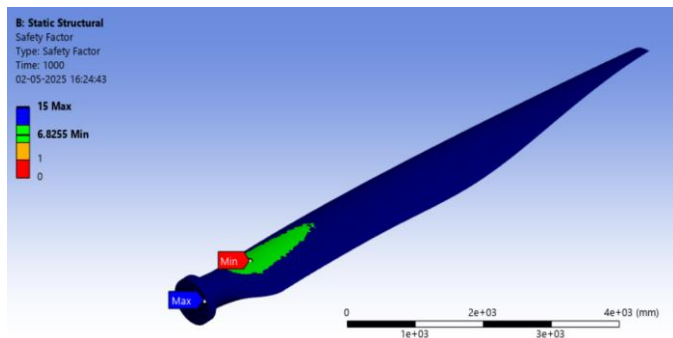


Figure 6.10- FOS- 6.8255

6.2. Modified Design

Applying carbon fibre material to the modified design with the increased thickness we get the following results of transient structural and static structural analysis.

i. Transient Structural Analysis:

- Max Pressure: 101325 Pa;
- Apply pressure on the blade and constraint the end locations i.e, holes
- Perform the analysis for 100 sec.

'Figure 6.11' shows that the pressure of 101325 Pa, which is atmospheric pressure, is applied on the face of the wind turbine blade and the bolting holes have been fixed for the transient structural analysis of the blade. The analysis is performed for 100 sec, and the results are as shown below.

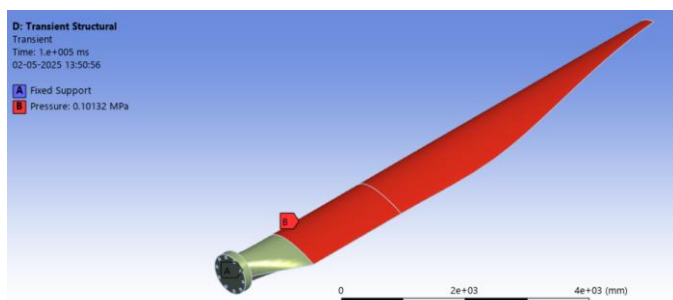


Figure 6.11- Transient Structural Analysis loading on Blade

Output:

- Stress

'Figure 6.12' shows that the minimum stress developed during the transient structural analysis is 0.063784 MPa, it occurs at the tip of the wind turbine blade. Whereas maximum stress developed during the transient stress analysis is 421.8 MPa, it occurs at the neck of the blade.

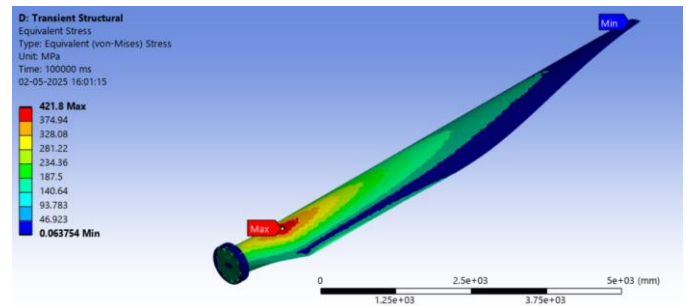


Figure 6.12- Von-Mises Stress- 421.8 MPa

- Deformation

'Figure 6.13' shows that the minimum deformation during the transient structural analysis is 0mm, it occurs at the bolting holes of the wind turbine blade. Whereas maximum deformation during the transient stress analysis is 473.82mm, it occurs at the tip of the blade.

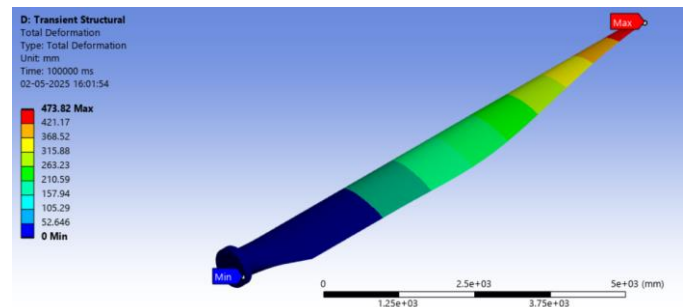


Figure 6.13- Deformation- 473.82mm

- Strain

'Figure 6.14' shows that the minimum strain during the transient structural analysis is 4.6161×10^{-7} , it occurs at the tip of the wind turbine blade. Whereas maximum strain during the transient stress analysis is 0.00363, it occurs at the neck of the blade.

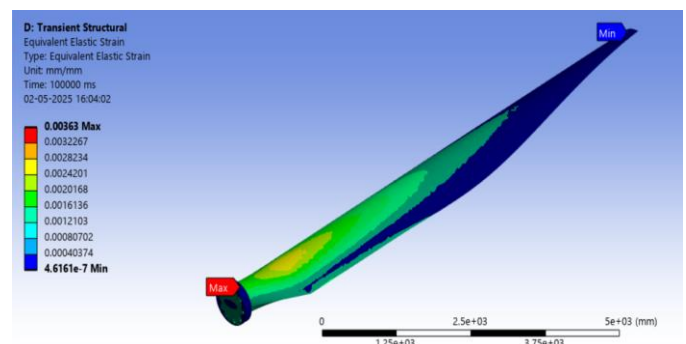


Figure 6.14- Strain- 0.00363

- FOS

'Figure 6.15' shows that the minimum factor of safety during the transient structural analysis is 10.669, it occurs at the neck of the wind turbine blade. Whereas maximum

factor of safety during the transient stress analysis is 15, it occurs at the bolting holes of the blade.

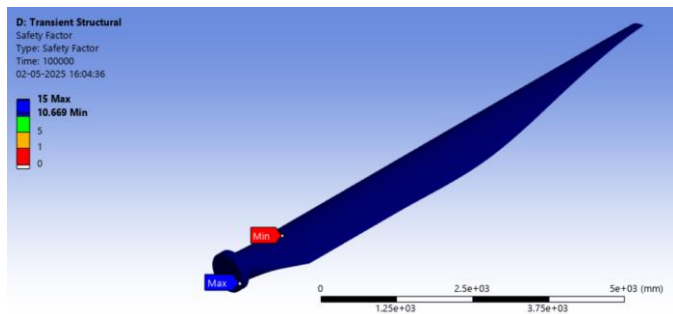


Figure 6.15- FOS- 10.669

ii. **Static Structural Analysis:**

- Max Pressure: 101325 Pa;
- Apply pressure on the blade and constraint the end locations i.e., holes

'Figure 6.16' shows that the pressure of 101325 Pa, which is atmospheric pressure, is applied on the face of the wind turbine blade and the bolting holes are fixed for the static structural analysis of the blade. The results of the analysis are as shown below.

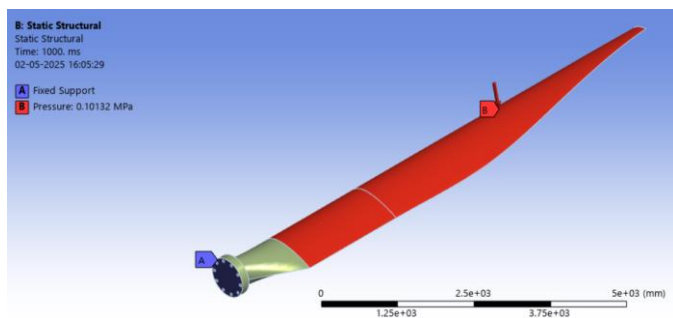


Figure 6.16- Static Structural Analysis loading on Blade

Output:

- Stress

'Figure 6.17' shows that the minimum stress developed during the static structural analysis is 0.063754 MPa, it occurs at the tip of the wind turbine blade. Whereas maximum stress developed during the transient stress analysis is 422.01 MPa, it occurs at the neck of the blade.

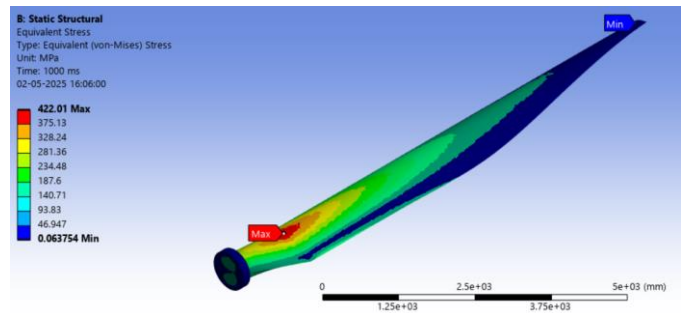


Figure 6.17- Von-Mises Stress- 422.01 MPa

- Deformation

'Figure 6.18' shows that the minimum deformation during the static structural analysis is 0mm, it occurs at the bolting holes of the wind turbine blade. Whereas maximum deformation during the transient stress analysis is 470.71mm, it occurs at the tip of the blade.

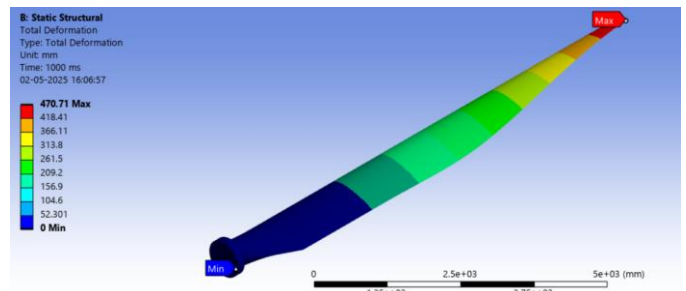


Figure 6.18- Deformation- 470.71mm

- Strain

'Figure 6.19' shows that the minimum strain during the static structural analysis is 4.6162×10^{-7} , it occurs at the tip of the wind turbine blade. Whereas maximum strain during the transient stress analysis is 0.00282, it occurs at the neck of the blade.

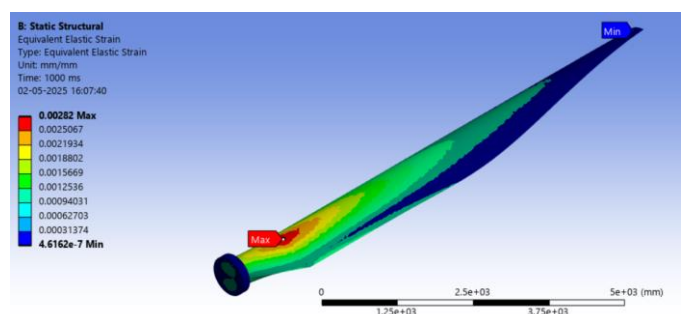


Figure 6.19- Strain- 0.00282

- FOS - 10.663

'Figure 6.20' shows that the minimum factor of safety during the static structural analysis is 10.663, it occurs at the neck of the wind turbine blade. Whereas maximum

factor of safety during the transient stress analysis is 15, it occurs at the bolting holes of the blade.

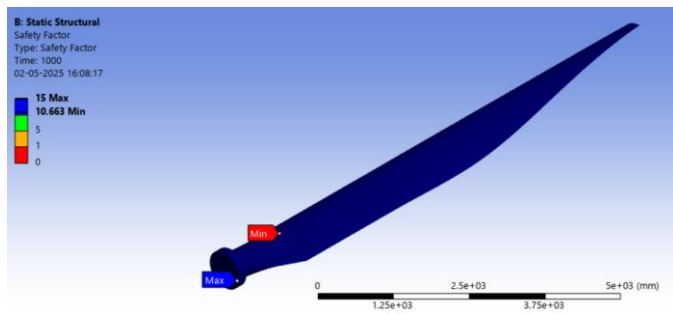


Figure 6.20- FOS- 10.663

7. Results

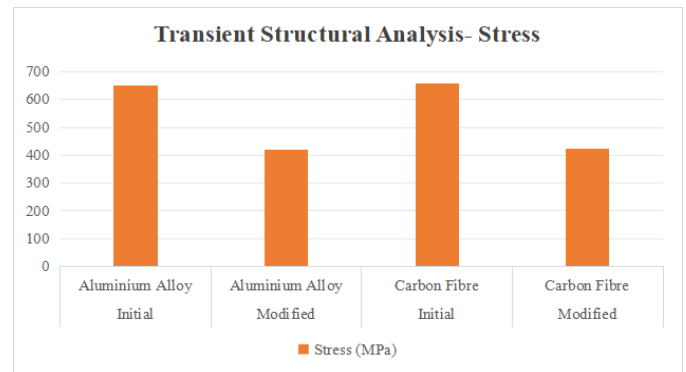
The following 'Table 7.1' shows the comparison between both the initial and the modified designs for aluminium alloy as well as for the carbon fibre material available. We can see from the results that there is no significant difference in stress when the material is changed. However, the deformation goes on decreasing as we move in the rows, similar thing can be seen for the strain as well. We can notice that there is a huge difference in the factor of safety between the aluminium alloy and the carbon fibre materials. Similar patterns can be observed for both the transient structural as well as static structural analysis.

	Design	Initial	Modified	Initial	Modified
	Material	Al Alloy	Al Alloy	Carbon Fibre	Carbon Fibre
TSA	Stress (MPa)	649.12	418.63	658.43	421.8
	Deform (mm)	1894.4	980.44	908.49	473.82
	Strain	0.0091	0.0072	0.0044	0.0036
	FOS	0.43135	1.0749	6.8344	10.669
SSA	Stress (MPa)	652.35	419.21	659.3	422.01
	Deform (mm)	1904.1	974.05	908.72	470.71
	Strain	0.0092	0.0058	0.0044	0.0028
	FOS	0.42922	1.0734	6.8255	10.663

Table 7.1- Structural Analysis Results

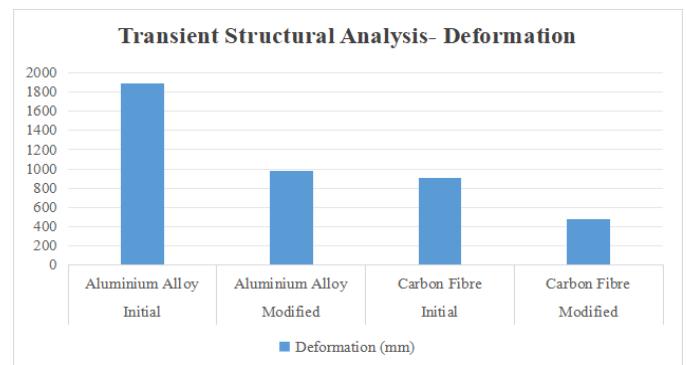
'Graph 7.1' below shows the Von Mises stresses developed in the wind turbine blade during the transient structural

analysis. We can see that the modified blade design with aluminium alloy has the least maximum stress developed, whereas the initial blade design with carbon fibre material has the most maximum stress developed.



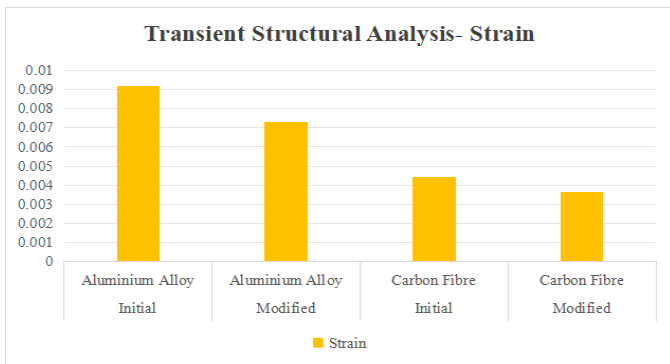
Graph 7.1- Transient Structural Analysis- Stress Results

'Graph 7.2' below shows the deformation in the wind turbine blade during the transient structural analysis. We can see that the initial blade design with aluminium alloy has the most deformation, whereas the modified blade design with carbon fibre material has the least deformation.



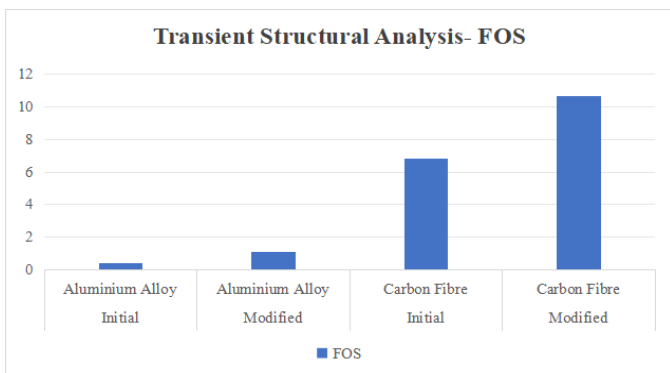
Graph 7.2- Transient Structural Analysis- Deformation Results

'Graph 7.3' below shows the strain in the wind turbine blade during the transient structural analysis. We can see that the initial blade design with aluminium alloy has the most strain, whereas the modified blade design with carbon fibre material has the least strain.



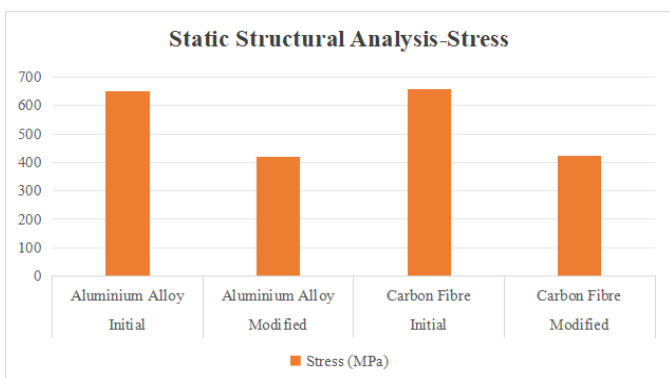
Graph 7.3- Transient Structural Analysis- Strain Results

'Graph 7.4' below shows the FOS in the wind turbine blade during the transient structural analysis. We can see that the initial blade design with aluminium alloy is least safe, whereas the modified blade design with carbon fibre material is the safest.



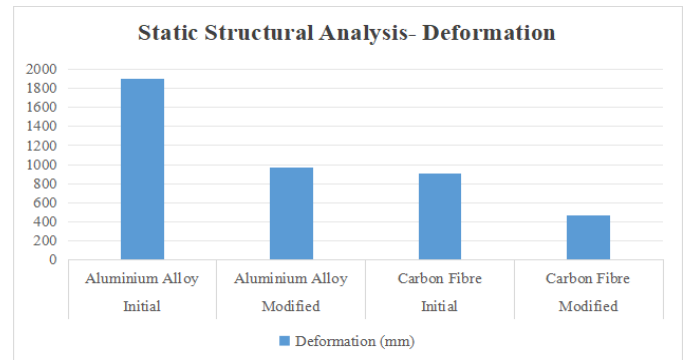
Graph 7.4- Transient Structural Analysis- FOS Results

'Graph 7.5' below shows the Von Mises stresses developed in the wind turbine blade during the static structural analysis. We can see that the modified blade design with aluminium alloy has the least maximum stress developed, whereas the initial blade design with carbon fibre material has the most maximum stress developed.



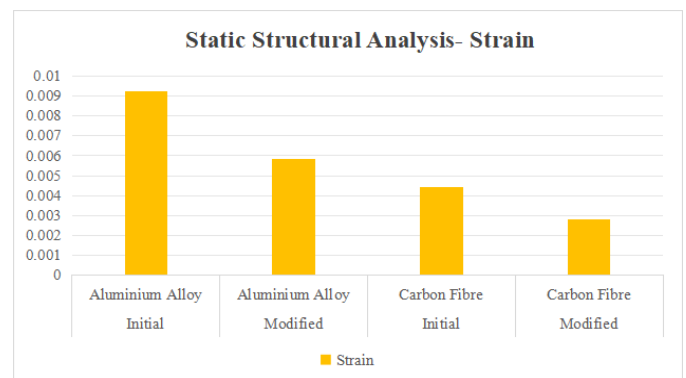
Graph 7.5- Static Structural Analysis- Stress Results

'Graph 7.6' below shows the deformation in the wind turbine blade during the static structural analysis. We can see that the initial blade design with aluminium alloy has the most deformation, whereas the modified blade design with carbon fibre material has the least deformation.



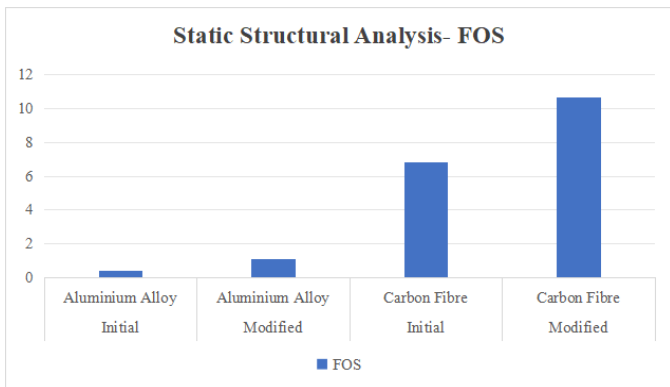
Graph 7.6- Static Structural Analysis- Deformation Results

'Graph 7.7' below shows the strain in the wind turbine blade during the transient structural analysis. We can see that the initial blade design with aluminium alloy has the most strain, whereas the modified blade design with carbon fibre material has the least strain.

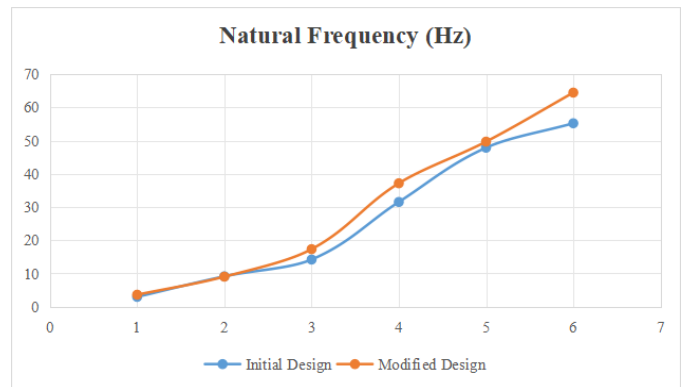


Graph 7.7- Static Structural Analysis- Strain Results

'Graph 7.8' below shows the FOS in the wind turbine blade during the transient structural analysis. We can see that the initial blade design with aluminium alloy is least safe, whereas the modified blade design with carbon fibre material is the safest.



Graph 7.8- Static Structural Analysis- FOS Results



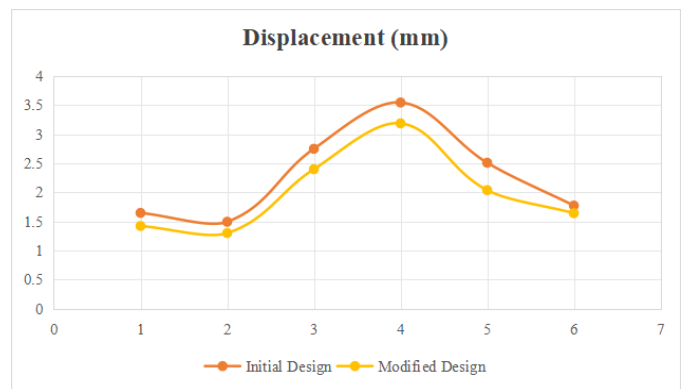
Graph 7.9- Frequency Results

The following 'Table 7.2' shows the comparison between first six modes of vibration or natural frequency for both the designs of the aerofoil available for the aluminium alloy. We can see that the initial modes of the natural frequency are very close to each other, whereas they move far from each other as we move ahead in the modes of frequency.

'Graph 7.10' below shows the displacement of the first six modes in the wind turbine blade during the modal analysis. We can see that the displacements for the modes are almost parallel to each other, peaking at the mode 4.

Table 7.2- Modal Analysis Results

		Initial	Modified
Mode 1	Frequency (Hz)	2.961	3.61
	Displacement (mm)	1.6483	1.4233
Mode 2	Frequency (Hz)	9.14	9.0448
	Displacement (mm)	1.4954	1.3014
Mode 3	Frequency (Hz)	14.202	17.33
	Displacement (mm)	2.751	2.3998
Mode 4	Frequency (Hz)	31.533	37.166
	Displacement (mm)	3.5472	3.1889
Mode 5	Frequency (Hz)	47.869	49.699
	Displacement (mm)	2.5114	2.0397
Mode 6	Frequency (Hz)	55.224	64.456
	Displacement (mm)	1.7743	1.6436



Graph 7.10- Frequency Results

8. Conclusion

- The thickness-to-chord ratio in the optimized aerofoil is 27% which is in the optimal range.
- Thus we can conclude that the overall performance of the wind turbine blade has been enhanced.
- We can also conclude that the new design is stronger and safer to the structural loading for the same material as compared to the initial design.
- The modal analysis shows less deformation for the first six modes for the modified design as compared to the initial design.
- From the results we can also conclude that the carbon fibre material is stronger as compared to the aluminium alloy.
- Thus, we can say that carbon fibre is a safer material than aluminium alloy.

References

1. K.Y. Maalawi, M.A. Badr, A practical approach for selecting optimum wind rotors, *Renewable Energy*. 28 (2003) 803-822.
2. R.W. Thresher, D.M. Dodge, Trends in the evolution of wind turbine generator configurations and systems. *Wind Energy*, 1 (1998) 70–86.
3. J.L. Tangler, The Nebulous art of using wind-tunnel airfoil data for predicting rotor Performance, 5 (2002) 245-257.
4. Experimental modal analysis for WTS-3 wind turbine (1981). Report HSER 8205, Hamilton standard division of United Technologies Corporation.
5. Larsen, G.C. and Kretz, A. (1995). Experimental Determination of Stiffness Distributions and Mode Shapes of Wind Turbine Blades. Riso-R-773(EN).
6. Larsen, G. C., Hansen, M. H., Baumgart, A., & Carlén, I. (2002). Modal analysis of wind turbine blades. Denmark. Forskningscenter Risoe. Riso-R No. 1181
7. Dimitriadis E., Missirlis D. and Martinopoulos G. 2014 European Wind Energy Association, Barcelona.
8. Dhurpate P. R., Sutar K. B. and Kale S. A. 2016 Imp. J. Interdiscip. Res. 2(6)5.
9. Soland T. and Thuné S., 2012 Bachelor Thesis.
10. Kale S. A., Birajdar M. and Sapali S. N. 2016 J. Altern. Energy Sources Technol. 6(1).
11. Z.L. Mahri, M.S. Rouabah, "Calculation of dynamic stresses using finite element method and prediction of fatigue failure for wind turbine rotor" *Wseas Transactions On Applied And Theoretical Mechanics*, Issue 1, Volume 3, January 2008
12. Mickael Edon, "38 meter wind turbine blade design, internship report"
13. Philippe Giguere and Selig, "Blade Geometry Optimization For The Design Of Wind Turbine Rotors" AIAA-2000-0045
14. M. Jureczko, M. Pawlak, A. Mezyk, "Optimization of wind turbine blades", *Journal of Materials Processing Technology* 167 (2005) 463–471
15. Tingting Guo, Dianwen Wu, Jihui Xu, Shaohua Li, "The Method of Large-scale Wind Turbine Blades Design Based on MATLAB Programming", *IEEE*
16. Carlo Enrico Carcangiu, "CFD-RANS Study of Horizontal Axis Wind Turbines" ,Doctor of philosophy Thesis report
17. K.J.Jackson, et al., "Innovative design approaches for large wind turbine blades", 43rd AIAA Aerospace Sciences Meeting and Exhibit 10 - 13 January 2005, Reno, Nevada
18. Wang Xudong, et al., "Blade optimizations for wind turbines", *Wind Energy*. 2009;12:781–803, Published online 29 April 2009 in Wiley Interscience
19. Karam Y, Hani M, "Optimal frequency design of wind turbine blades", *Journal of Wind Engineering and Industrial Aerodynamics* 90 (2002) 961–986
20. Ming-Hung Hsu, "Vibration Analysis Of Pre-Twisted Beams Using The Spline Collocation Method", *Journal of Marine Science and Technology*, Vol. 17, No. 2, pp. 106-115 (2009) 74
21. S. S .Rao, R.K Gupta , " Finite Element Vibration Analysis Of Rotating Timoshenko Beams", *Journal of Sound and vibration* (2001) 242(1), 103}124
22. B. Hillmer et al., " Aerodynamic and Structural Design of Multi MW Wind Turbine Blades beyond 5MW", *Journal of Physics: Conference Series* 75 (2007) 012002
23. J.H.M. Gooden, "Experimental Lowe speed Aerodynamic Characteristics of the Wortmann FX 66-S-196 V1 Airfoil", <http://www.standardcirrus.org/FX66-S-196V1-Gooden.PDF>
24. Bharath Koratagere Srinivasa Raju 2011 "Design optimization of a wind turbine blade" The University of Texas at Arlington.
25. Miller, A.; Chang, B.; Issa, R.; Chen, G. Review of computer-aided numerical simulation in wind energy. *Renew. Sustain. Energy Rev.* **2013**, 25, 122–134.
26. Madsen, M.H.A.; Zahle, F.; Sørensen, N.N.; Martins, J.R. Multipoint high-fidelity CFD-based aerodynamic shape optimization of a 10 MW wind turbine. *Wind Energy Sci.* **2019**, 4, 163–192.
27. Horcas, S.G.; Ramos-García, N.; Li, A.; Pirrung, G.; Barlas, T. Comparison of aerodynamic models for horizontal axis wind turbine blades accounting for curved tip shapes. *Wind Energy* **2023**, 26, 5–22.
28. Batay, S.; Baidullayeva, A.; Zhao, Y.; Wei, D.; Baigarina, A.; Sarsenov, E.; Shabdan, Y. Aerostructural Design Optimization of Wind Turbine Blades. *processes* **2024**, 12, 22.

29. Jureczko, M.; Pawlak, M.; Mezyk, A. Optimisation of wind turbine blades. *J. Mater. Proc. Technol.* **2005**, *167*, 463–471.
30. Chattot, J.J. Optimization of wind turbines using helicoidal vortex model. *J. Sol. Energy Eng. Trans. ASME* **2003**, *125*, 418–424.
31. Fuglsang, P.; Madsen, H.A. Optimization method for wind turbine rotors. *J. Wind Eng. Ind. Aerodyn.* **1999**, *80*, 191–206.
32. Jureczko, M.; Pawlak, M.; Mezyk, A. Optimisation of wind turbine blades. *J. Mater. Proc. Technol.* **2005**, *167*, 463–471.
33. Schubel, Peter J., and Richard J. Crossley. 2012. "Wind Turbine Blade Design" *Energies* 5, no. 9: 3425-3449.